The influence of different diffusion pattern to the sub- and super-critical fluid flow in brown coal

Peihuo Peng[1, 2]

[1]School of Mechanics and Civil Engineering, China University of Mining & Technology, Beijing 100083, China

[2]School of Science, Beijing University of Civil Engineering & Architecture, Beijing 102612, China

*Correspongding Author

E-mail: pph773@bucea.edu.cn

Abstract. Sub- and super-critical CO_2 flowing in nanoscale pores are recently becoming of great interest due to that it is closely related to many engineering applications, such as geological burial and sequestration of carbon dioxide, Enhanced Coal Bed Methane recovery (ECBM), super-critical CO_2 fracturing and so on. Gas flow in nanopores cannot be described simply by the Darcy equation. Different diffusion pattern such as Fick diffusion, Knudsen diffusion, transitional diffusion and slip flow at the solid matrix separate the seepage behaviour from Darcy-type flow. According to the principle of different diffusion pattern, the flow of sub- and super-critical CO_2 in brown coal was simulated by numerical method, and the results were compared with the experimental results to explore the contribution of different diffusion pattern and swelling effect in sub- and super-critical CO_2 flow in nanoscale pores.

1. Introduction

China has become the world's first greenhouse gas emission country since 2008, facing enormous pressure of greenhouse gas emission reduction. Carbon dioxide Capture and Storage (CCS) technology has received more and more attention and concern in China. The Chinese government and many enterprises believe that CCS technology will play an important role in China's long-term CO_2 emission reduction strategy. CO_2 need to be compressed in order to achieve better geological sequestration effect. When the depth reaches or exceeds 800m, CO_2 will reach supercritical state. Environmental impact and risk is the focus of the geological sequestration of CO_2, it is possible that CO_2 will release slowly from the underground geological layer because of the seepage effect. So the seepage mechanism of supercritical CO_2 flowing in the underground reservoir has a very important significance on the CCS technology.

In coal beds, most CH_4 exists in an adsorbed phase in the coal matrix. Compared with CH_4, the adsorption capacity of CO_2 in reservoir is higher than that of CH_4, and CO_2 has better 'affinity' with the reservoir, injection of CO_2 into coal can 'replace' CH_4 adsorbed in the reservoir[1-4]. Researchers have also been studying the seepage mechanism of sub- and super-critical CO_2 in the coal seam to get better Coal Bed Methane recovery (CBM).

Hydraulic fracturing promoted the rapid development of shale gas, but also attracted controversy continuously, such as water pollution. And in addition to the threat to water resources, hydraulic fracturing has also encountered some other scientific and technical bottlenecks, which have limited its

application. To figure out these difficulties, researchers put forward the concept of supercritical CO_2 fracturing. Supercritical CO_2 fracturing is mainly the seepage-stress coupling problem of supercritical CO_2 in reservoir. So to understand the real seepage mechanism of supercritical CO_2 flowing in nanopores make a big step forward to the development of supercritical CO_2 fracturing.

There are different sizes of pores in coal seam, shale, tight rock, the lowest diameter is to the nanometer scale, which is close to molecular diameter of CO_2. Darcy's law is conventional method to research seepage problem in matrix with micron size or even bigger pores. But the Darcy equation are not suitable for seepage in nanopores. When gas flow in porous media, the ratio of mean-free-path of molecular motion and pore size is different, the interaction between gas molecules and pore wall changes, these interactions include: (1) mutual collisions between gas molecules; (2) collisions between gas molecules and pore walls. Different interactions result in different seepage mechanism. A widely recognized dimensionless parameter Knudsen number *Kn* is usually used to determine the type of seepage mechanism. It is a characteristic physical quantity represent what kind of collision frequency is mainly more higher, the collisions between molecules or the collisions between nanapore walls and molecules? Knudsen number is defined as the ratio of the fluid mean-free-path and the diameter of the pore size.

According to Knudsen number *Kn*, seepage mechanisms can be divided into: Knudsen diffusion, Fick diffusion and Transitional diffusion. When the Knudsen number $Kn \geq 10$, mean-free-path of gas molecular is greater than the pore diameter, collisions between gas molecules and pore walls play a major role (Figure 1), such flow called Knudsen diffusion.

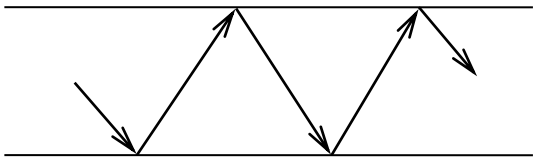

Figure 1: Knudsen diffusion ($Kn \geq 10$)

When the Knudsen number $Kn \leq 0.1$, the pore diameter is far bigger than the mean free path of gas molecular, the collisions between free gas molecules play a major role (Figure 2), this kind of diffusion called Fick's diffusion.

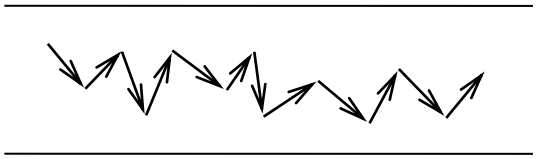

Figure 2: Fick diffusion ($Kn \leq 0.1$)

When the Knudsen number $0.1 < Kn < 10$, size of pore diameter and mean free path of gas molecule are almost same, collisions between the free molecules and collisions between molecules and the pore walls are equally important (Figure 3), it is called transitional diffusion.

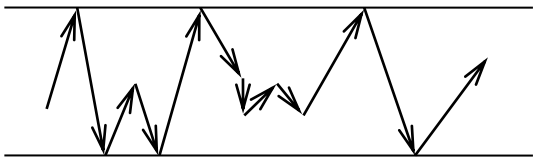

Figure 3: Transitional diffusion ($0.1 < Kn < 10$)

In the study of seepage problem of coal seam or shale, pore size will changes in different scales. Pressure of fluid change and also temperature change due to the heat exchange, the Knudsen number *Kn* will varies in a number of different ranges, which caused diffusion pattern changing from the Knudsen diffusion ,Transitional diffusion, to the Fick diffusion. We studied the seepage mechanism in the porous matrix with nanopores uniformly distributed, established a seepage simulation model that is

suitable for diffusion pattern continuous changing with pressure at the same temperature, and solved the model by the numerical method, analyzed the influence of different diffusion mechanisms to seepage results, and in the numerical model the slip flow effect and swelling effect are also considered. At last, the numerical results are compared with the experimental results.

2. Model Description

The model is based on the following assumptions: (1) There is only a single phase single component gas migration in rock matrix; (2) ignore the effect of gravity on seepage, reservoir temperature remains unchanged during gas migration; (3) The rock matrix is regarded as porous media with uniform pore distribution, and the pores size is nanometer scale.

The equations of mass flux in the process of gas molecules migration in nanopores is as following, it is the result of a combination of pressure forces and diffusion[5]:

$$J = J_a + J_D \tag{2.1}$$

where J is the total mass flux. The first term on the right-hand side is advective flow due to pressure force, the second term is Knudsen diffusion, Transitional diffusion, or Fick diffusion.

The mass flux of advective flow J_a is given by Hagen Poiseuille's equation[5, 6]:

$$J_a = -\frac{r^2}{8\mu}\rho\frac{\Delta p}{L} \tag{2.2}$$

Where r is the radius of the pore, μ is fluid viscosity, ρ is the density of the gas fluid.

And the mass flux of gas diffusion is given by:

$$J_D = -\frac{MD}{RT}\frac{\Delta p}{L} \tag{2.3}$$

In which M is molar mass, R (=8.314 J/mol/K) is the gas constant, T is absolute temperature in Kelvin, D is the diffusional coefficient.

When calculate the mass flux of fluid diffusion in porous media, first determine the diffusion type according to the Knudsen number, and obtain the diffusion coefficient of the corresponding diffusion pattern. In fact, the diffusion coefficient D is a function of Knudsen number, namely the function of molecular mean free path and pore size.

2.1 Calculation of Knudsen Number Kn

The Knudsen number is the spatial field function in this model, which changes with the spatial position. The Knudsen number is locally different in the whole flow field, the local Knudsen number is a measure of the degree of rarefaction of gas molecules encountered through nanosize pores, which determines the different diffusion mode.

Knudsen number is defined as the fluid mean-free-path divided by the diameter of the pore.

$$K_n = \frac{\lambda}{d_n} \tag{2.4}$$

Where Kn is Knudsen number, it is dimensionless. d_n is the diameter of the pore, λ is the fluid mean-free-path, it is commonly calculated by the following formula[7]:

$$\lambda = \frac{k_B T}{\sqrt{2}\pi\delta^2 P} \tag{2.5}$$

In which k_B is the Boltzmann constant (1.3805×10^{-23}J/K), T is absolute temperature in Kelvin, P is pressure and δ is the collision diameter of the gas molecule.

The mean free path of gas can also be computed by the Loeb method for an ideal gas, calculating formula of mean free path is following[8]:

$$\lambda = \sqrt{\frac{\pi RT}{2M}}\frac{\mu_g}{P} \tag{2.6}$$

Where M is molar mass, R (=8.314 J/mol/K) is the gas constant, μ_g is fluid viscosity.

2.2 Diffusion coefficients of different kinds of diffusion pattern

2.2.1 Knudsen diffusion

According to molecular dynamics theory, the calculation formula of Knudsen diffusion coefficient is

following:

$$D_{Knudsen} = \frac{2r}{3}\sqrt{\frac{8RT}{\pi M}} \quad (2.7)$$

Where $D_{Knudsen}$ is the Knudsen diffusion coefficient. M is molar mass, R (=8.314 J/mol/K) is the gas constant, T is absolute temperature in Kelvin.

2.2.2 Fick diffusion

In Fick's diffusion, collisions between the molecules of the fluid is the main type collision when gas flow in rock medium, and the collisions between the pore walls and the molecules can neglect, it is similar to the situation in the pure liquid, the Fick diffusion coefficient can be calculated by the Stokes-Einstein equation.

$$D_{fick} = \frac{k_B T}{6\pi\mu_B r_A} \quad (2.8)$$

Where D_{fick} is the Fick's diffusion coefficient, r_A is the radius of the gas molecules, μ_B is viscosity of the fluid contained in the pore, k_B is the Boltzmann constant, it is the absolute gas constant divided by the Avogadro number, namely $k_b = R/N_A = 8.314 \div (6.02 \times 10^{23}) = 1.38 \times 10^{-23}$, T is absolute temperature in Kelvin.

2.2.3 Transitional diffusion

Transitional diffusion coefficient is combined by Knudsen diffusion coefficient and Fick diffusion coefficient:

$$D_{Transitional} = ({D_{Knudsen}}^{-1} + {D_{fick}}^{-1})^{-1} \quad (2.9)$$

2.3 The slip flow effect

The seepage characteristics of gas in porous media is different from that of liquid, gas in the pores does not produce thin adsorption layer, the flow velocity of the gas fluid at the pore walls is not zero. For very small pores at the nanoscale, the no-slip boundary condition is sometimes invalid[9, 10]. This characteristic is called slip flow effect.

There exists slip flow effect when fluid flow in nanosize pores, a dimensionless factor can be introduced to adjust the equation of Hagen-Poiseuiue[5]:

$$J_a = -k_s \frac{r^2}{8\mu}\rho_{avg}\frac{\Delta p}{L} = -[1 + \sqrt{\frac{8\pi RT}{M}}\frac{\mu}{p_{avg}}\left(\frac{2}{\alpha} - 1\right)]\frac{r^2}{8\mu}\rho_{avg}\frac{\Delta p}{L} \quad (2.10)$$

k_s is correction coefficient for the slip flow effect, it is dimensionless; α is tangential momentum accommodation coefficient, it is related to these factors, such as pressure, temperature, the roughness of the pore walls and type of gas, its value can be measured with the range 0 to 1. it is assumed to be 0.5 in this study.

If the ambient temperature is constant, the size and distribution of the matrix pores are uniform, when the seepage flow reaches the steady state, the mass flux through each section is equal, and it is not related to the time. It can be expressed as a differential form in 1D problem according to the above description:

$$J = \left(-\frac{M}{RT}D(p) - \frac{r^2}{8}\frac{\rho}{\mu} - \frac{r^2}{8}\rho\sqrt{\frac{8\pi RT}{M}}(\frac{2}{\alpha} - 1)\frac{1}{p}\right)\frac{dp}{dx} = Constant \quad (2.11)$$

We get a two-order differential equation by taking derivative of the above function.

$$\left(-\frac{M}{RT}D(p) - \frac{r^2}{8}\frac{\rho}{\mu} - \frac{r^2}{8}\rho\sqrt{\frac{8\pi RT}{M}}(\frac{2}{\alpha} - 1)\frac{1}{p}\right)\frac{d^2p}{dx^2} + \frac{r^2}{8}\rho\sqrt{\frac{8\pi RT}{M}}\left(\frac{2}{\alpha} - 1\right)\frac{1}{p^2}\left(\frac{dp}{dx}\right)^2 = 0 \quad (2.12)$$

$D(p)$ is diffusion coefficient function of pressure. According to the above, the expression of $D(p)$ is as follows:

$$D(p)=\begin{cases}\frac{2r}{3}\sqrt{\frac{8RT}{\pi M}}, & when \quad p\le\frac{k_BT}{10\sqrt{2}\pi\delta^2d_n}\\ \frac{4\sqrt{2R}rk_BT}{3k_B\sqrt{\pi MT}+24\pi\sqrt{2R}\mu_Br_Ar}, & when \quad \frac{k_BT}{10\sqrt{2}\pi\delta^2d_n}<p<\frac{10k_BT}{\sqrt{2}\pi\delta^2d_n}\\ \frac{k_BT}{6\pi\mu_Br_A}, & when \quad p\ge\frac{10k_BT}{\sqrt{2}\pi\delta^2d_n}\end{cases} \tag{2.13}$$

In the above seepage type, if boundary conditions are known, the pressure field can be calculated, the obtained pressure field are substituted into the equations, the entire model is solved, such as permeability, mass flux and so on.

3. Numerical Method

In the above differential equations, $D(p)$ is a piecewise function, the analytic solution is difficult to get . The full implicit finite difference method is used to solve the differential equation with MATLAB. When solving, first calculate the mean free path according to the pressure, then get the Knudsen number, determine the type of diffusion, and then apply the corresponding formula for the diffusion coefficient.

Figure 4 shows a simplified flow chart of solution procedure. The algorithm is composed of six parts:

(1) The Model definition part do the assignment of the constant parameters and initializes all variables.

(2) Discretization part discretize the continuous pressure function to array $p_i(x_i)(i=0,1,\cdots n)$, the coordinates of x_i are $x_i=\frac{i\cdot L}{n}$, step size is $\frac{L}{n}$.

(3) Diffusion model estimation part to calculate the correlation coefficient and the critical pressure of the diffusion mode conversion.

(4) Tentative conversion point test section to estimate the possible diffusion patterns according to the boundary conditions, and a certain x_{k1} is assumed to be the transition point of different diffusion patterns.

(5) Diffusion coefficients calculated by different diffusion models in different regions. And then the Solver part solves the functions.

(6) Results judge part analyze the results, if $p_{k1}(x_{k1})>p_{cr}+\varepsilon$, then do the downstream traversal, to find the closest $p_{k2}(x_{k2})$ to the p_{cr} in the results, do assignment of $x_{k1}=x_{k2}$, go to the fourth step to do cycle calculation; if $p_{k1}(x_{k1})<p_{cr}-\varepsilon$, then do the upstream traversal, to find the closest $p_{k2}(x_{k2})$ to the p_{cr} in the results, do assignment of $x_{k1}=x_{k2}$, go to the fourth step to do cycle calculation; if $|p_{k1}(x_{k1})-p_{cr}|\ll\varepsilon$, successfully solved , end the solution procedure.

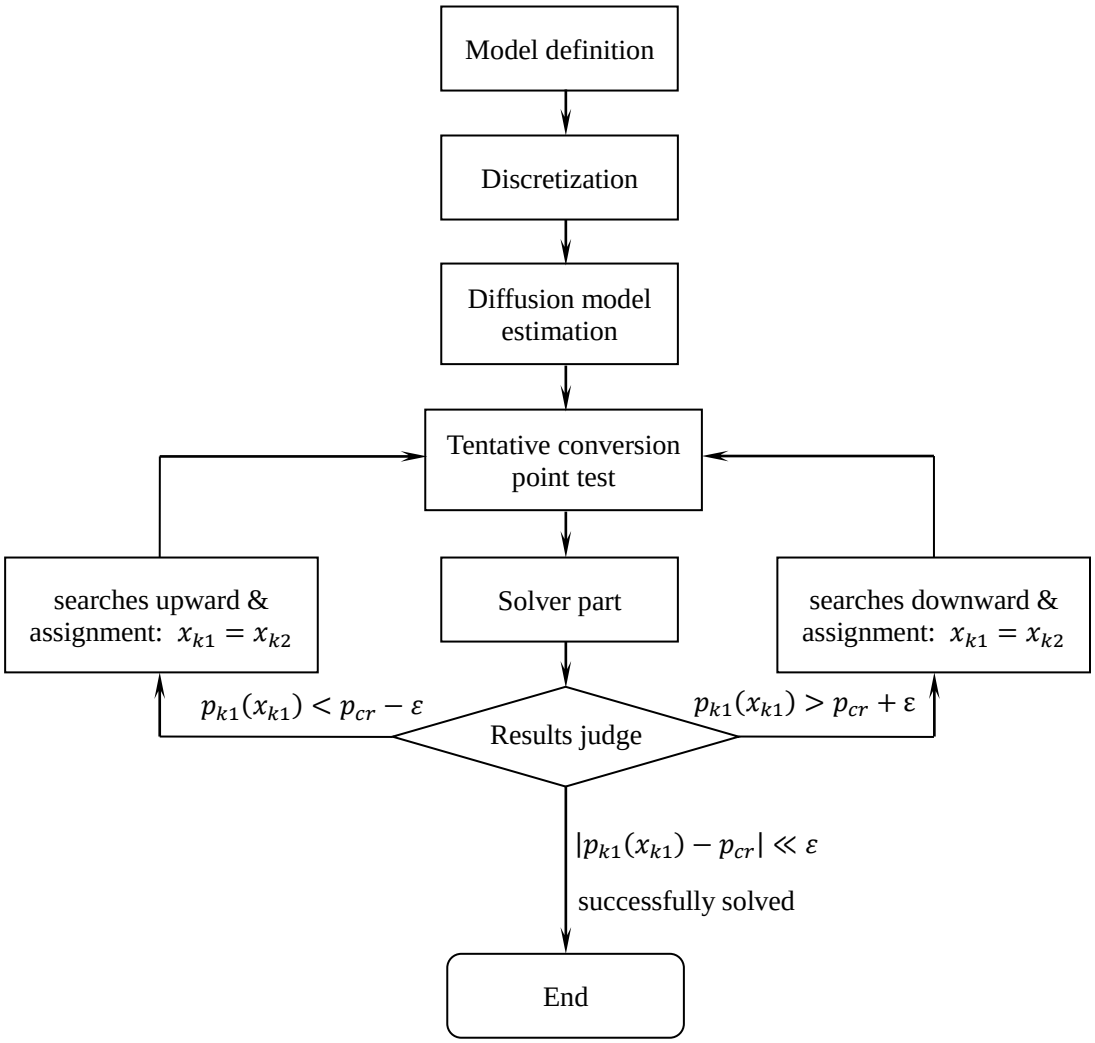

Figure 4: The flow chart of solution procedure

Some important parameters in the model are listed in Table 1.

Table 1 Values of parameters in simulator[11-14]

Symbol	Meaning	Parameter value
T	matrix temperature	311 K(38℃)
M_{CO2}	molar mass of CO_2	44×10^{-3} kg/mol
M_{N2}	molar mass of N_2	28×10^{-3} kg/mol
R	gas constant	8.314 J/mol/K
r	radius of the pores	1.3nm
ρ_{CO2}	density of CO_2	304kg/m^3
ρ_{N2}	density of N_2	133 kg/m^3
μ_{CO2}	viscosity of CO_2	20 μ Pa.s
μ_{N2}	viscosity of N_2	21 μ Pa.s
α	tangential momentum accommodation coefficient	0.5
k_B	Boltzmann constant	1.3805×10^{-23}J/K
r_{CO2}	radius of CO_2 molecule	0.165nm
r_{N2}	radius of N_2 molecule	0.18nm
δ_{CO2}	collision diameter of CO_2	0.33nm
δ_{N2}	collision diameter of N_2	0.36nm
d_n	diameter of the pores	2.6nm

According to the above model, the ratio of the pressure-driven advective mass flux and the diffusional mass flux can be calculated. For N_2, if pressure changes from 0 to 10 MPa, when $p \leq \frac{k_B T}{10\sqrt{2}\pi\delta^2 d_n}$, substitute the above parameters into the formulas, $J_a/J_D = 0.29$. At this time, the diffusional mass flux is dominated. When $p > \frac{k_B T}{10\sqrt{2}\pi\delta^2 d_n}$, substitute the above parameters into the formulas, $J_a/J_D = 2.05$. In this condition, the pressure-driven advection mass flux is dominated. For CO_2, if pressure changes from 0 to 10 MPa, when $p \leq \frac{k_B T}{10\sqrt{2}\pi\delta^2 d_n}$, substitute the above parameters into the formulas, $J_a/J_D = 0.56$. At this time, the diffusional mass flux is dominated. When $p > \frac{k_B T}{10\sqrt{2}\pi\delta^2 d_n}$, substitute the above parameters into the formulas, $J_a/J_D = 3.31$. In this condition, the pressure-driven advection mass flux is dominated.

4. Numerical Results vs. Experimental Results

The pressure change law of CO_2 and N_2 in coal is calculated with this model, the numerical results are compared with the experimental data from literature[13]. In the process of making samples[13], the coal blocks were first broken into smaller pieces and then crushed into dust, the sample of this powdered coal was compacted under 11 MPa axial stress. So it is consistent with the assumptions, the numerical results are shown in Figure 5 and Figure 6. Figure 7-9 are respectively the pressure variation of N_2 seepage the first time, the pressure variation of CO_2 seepage, the pressure variation of N_2 second time. It can be seen that the numerical results and the experimental results are close to each other for the first time N_2 flow and CO_2 seepage, the numerical results and experimental results for the second N_2 flow differ far away. This is because of the swelling effect of supercritical CO_2, resulting in the structure reconstruction of coal sample, it has been inconsistent with the assumptions of the model.

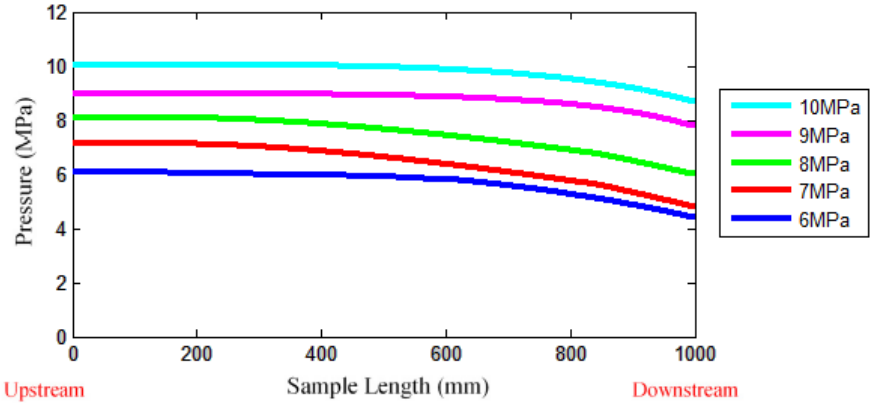

Figure 5: Pressure change law of N_2 flowing along the length of the sample

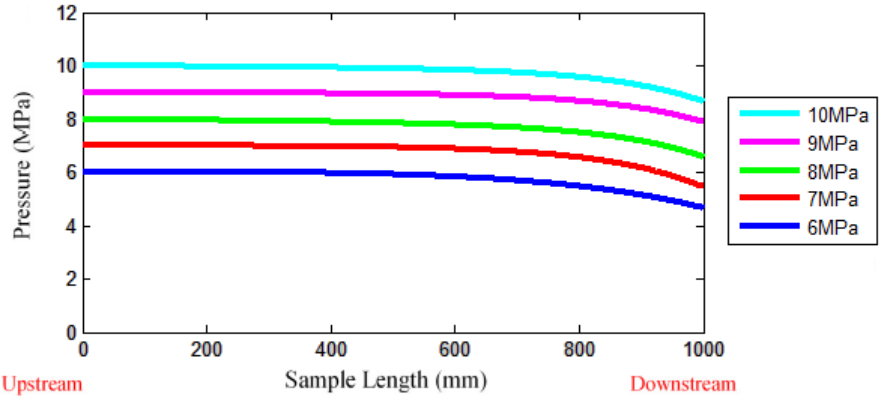

Figure 6: Pressure change law of CO_2 flowing along the length of the sample

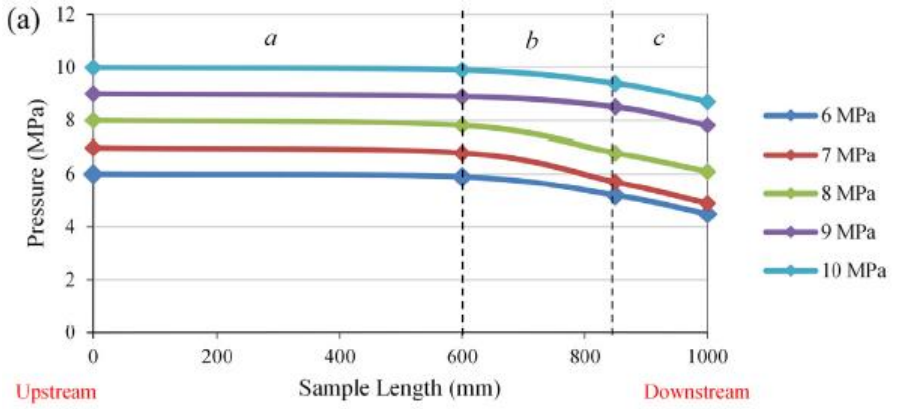

Figure 7: Pressure profiles for different injection pressures in first N_2 injection

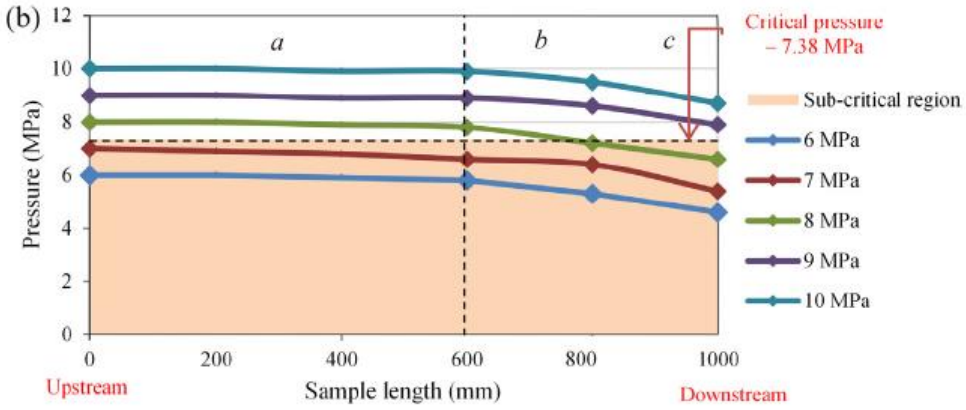

Figure 8: Pressure profiles for different injection pressures in CO_2 injection

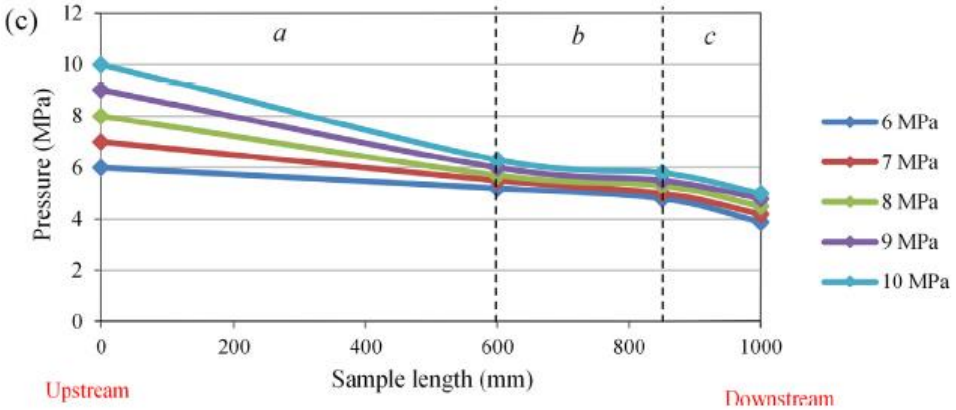

Figure 9: Pressure profiles for different injection pressures in second N_2 injection

5. Discussion and Conclusion

The total mass flux is the result of a combination of pressure forces and diffusion, and the phenomena of gas flow in nanoscale pores are composed of different controlling processes. In the pores of micron or above dimensions, diffusion effect can be ignored. However, numerical simulation analysis shows that advective flow due to pressure forces is much smaller compared with the diffusion, and diffusion which is negligible for conventional systems is the main transport mechanism and controls the gas flow in nanosize pores.

The numerical simulation of gas flow in nanopores of coal matrix was carried on in accordance with the relevant experimental parameters. Numerical results show that the diffusion patterns will change, the diffusion coefficient $D(p)$ decreases when Knudsen diffusion transformed into

transitional diffusion. When the experiment was just started, N_2 or CO_2 in the upper part of the sample is in the transitional diffusion pattern, and the lower part is in the Knudsen diffusion, with the rise of downstream pressure, diffusion pattern was transformed into the transitional diffusion in the whole sample. Thus, in the whole process of seepage, the ratio of the mass flux due to diffusion to total mass flux was changing. Because the final results of the experiments is the pressure profiles after 24 hours, the pressure development downstream becomes steady by 24h of injection, therefore the pressure development throughout the sample can be considered as the ultimate pressure distribution along the sample. The seepage state can be regarded as the steady flow, so the total mass flux remains constant.

But from the comparison of numerical results and experimental results, which has a certain deviation. There may be several reasons for the deviation between numerical results and experimental results:

(1) Although the experimental data acquisition time is 24 hours later, the pressure change with time is very small, the seepage is close to the steady state, but it is not the steady state yet, the mass flux is not constant, so there is a certain error of the above methods.

(2) CO_2 adsorption-induced coal matrix swelling creates significant changes to the fluid flow behavior in coal. The numerical results and the experimental results of the second N_2 injection are very far. Because of the greater internal structural modification caused by swelling of the supercritical CO_2 on coal sample, the coal mass structure has already been critically reformed and rearranged during the CO_2 flood. The diameter of the pores is no longer single size, and pores distribution is not uniform. The model assumptions were not satisfied, so the numerical results differ far with the experimental results.

(3) The adsorption-desorption effect of CO_2 on mass transfer was not considered in the flow process of nanopores.

Acknowledgments
This study is supported by the Science Project Foundation of Beijing Municipal Education Commission (SQKM201710016013), Science Research Foundation of BUCEA (00331616030).

References

[1] Z. Jin, A. Firoozabadi. *Methane and carbon dioxide adsorption in clay-like slit pores by Monte Carlo simulations*[J]. Fluid Phase Equilibria. 2013;360:456-65.
[2] Z. Jin, A. Firoozabadi. *Effect of water on methane and carbon dioxide sorption in clay minerals by Monte Carlo simulations*[J]. Fluid Phase Equilibria. 2014;382:10-20.
[3] R. Middleton, H. Viswanathan, R. Currier, R. Gupta. *CO_2 as a fracturing fluid: Potential for commercial scale shale gas production and CO_2 sequestration*[J]. Energy Procedia. 2014;63:7780-4.
[4] J. Li, X. Yan, W. Wang, Y. Zhang, J. Yin, S. Lu, et al. *Key factors controlling the gas adsorption capacity of shale: A study based on parallel experiments*[J]. Applied Geochemistry. 2015;58:88-96.
[5] F. Javadpour. *Nanopores and Apparent Permeability of Gas Flow in Mudrocks (Shales and Siltstone)*[J]. Journal of Canadian Petroleum Technology. 2009;48:16-21.
[6] S. Roy, R. Raju, H. F. Chuang, B. A. Cruden, M. Meyyappan. *Modeling gas flow through microchannels and nanopores*[J]. Journal of Applied Physics. 2003;93:4870.
[7] F. Javadpour, D. Fisher, M. Unsworth. *Nanoscale Gas Flow in Shale Gas Sediments*[J]. Journal of Canadian Petroleum Technology. 2007;46:55-61.
[8] L. Mi, H. Jiang, J. Li, L. Tao. *Mechanism of the Gas Diffusion in Shale Reservoirs*[J]. Petroleum Geology and Oilfield Development in Daqing. 2014;33:154-9. (In Chinese)
[9] N. G. Hadjiconstantinou. *The Limits of Navier-Stokes Theory and Kinetic Extensions for Describing Small Scale Gaseous Hydrodynamics*[J]. Physics of Fluids. 2006;18:111301-20.
[10] G. Karniadakis, A. Beskok, N. Aluru. *Microflows and Nanoflows: Fundamentals and Simulation*[M]. New York: Springer Science & Business Media, Inc.; 2005.

[11] G. Eris, A. A. Bozkurt, A. Sunol, A. Jonáš, A. Kiraz, B. E. Alaca, et al. *Determination of viscosity and density of fluids using frequency response of microcantilevers*[J]. The Journal of Supercritical Fluids. 2015;105:179-85.
[12] A. R. H. Goodwin. *A MEMS Vibrating Edge Supported Plate for the Simultaneous Measurement of Density and Viscosity: Results for Argon, Nitrogen, and Methane at Temperatures from (297 to 373) K and Pressures between (1 and 62) MPa*[J]. Journal of Chemical and Engineering Data. 2009;54:536-41.
[13] A. S. Ranathunga, M. S. A. Perera, P. G. Ranjith, Y. Ju. *A macro-scale experimental study of sub- and super-critical CO_2 flow behaviour in Victorian brown coal*[J]. Fuel. 2015;158:864-73.
[14] C. Li. *Advances in the Science of Victorian Brown Coal*[M]. Elsevier Science & Technology; 2004.